Arch Appl Mech (2015) 85:1363–1381
DOI 10.1007/s00419-014-0963-6

SPECIAL

Haris Alexakis · Nicos Makris

Limit equilibrium analysis of masonry arches

Received: 19 March 2014 / Accepted: 31 July 2014 / Published online: 26 November 2014
© Springer-Verlag Berlin Heidelberg 2014

Abstract In this paper, we revisit the limit equilibrium analysis of masonry arches. Firstly, the major contributions during the last three centuries associated with geometric and energy formulations are discussed, and subsequently, the paper explains that the problem of determining the minimum thickness of a masonry arch capable to support its own weight has multiple solutions. The infinite many neighboring solutions for the minimum thickness of a masonry arch result from the infinite many possible directions of rupturing that an arch with finite thickness may develop when becoming a mechanism. Given this infinite number of physically admissible rupturing directions, the energy approach expressed with the principle of stationary potential energy emerges as the most powerful tool to analyze masonry arches at their limit equilibrium state. The paper concludes that vertical rupturing is the most critical rupturing direction since it results to the largest value of the minimum thickness that an elliptical arch needs to support its own weight. For the common case where there is an intrados layer of voussoirs with physical joints perpendicular to the intrados, the initial rupture has to first follow the physical joint; therefore, the broken rupture pattern reported by Lamé and Clapeyron in 1823 corresponds to the larger value of the minimum allowable thickness.

Keywords Stone arches · Stereotomy · Line of resistance · Funicular polygon · Hinged mechanism · Variational formulation

1 Introduction

During the last three decades, we have witnessed a growing interest regarding the preservation of our cultural heritage and the retrofit of historic structures. The long history of these structures, most of them built out of masonry, is partly due to their sound structural configuration, the advanced level of construction practices and the quality of building materials. At the same time, the long loading history on these structures ranging from ground settlements to earthquake excitations has resulted in the accumulation of a variety of deformations which are responsible for a prevailing stress field that its current state may be challenging to assess.

In view of the challenge to assess the actual local stresses in a historic structure, which through the centuries has suffered a variety of deformation, an "elastic stress" analysis becomes less attractive, whereas the pretwentieth century "limit equilibrium" analysis has become again increasingly popular (Sinopoli et al. [1], Foce and Aita [2], De Luca et al. [3], among others).

During a limit state analysis, the various collapse mechanisms are first identified, and with simple calculations which derive primarily from energy methods, one can conclude whether the various rigid portions of the

H. Alexakis · N. Makris (✉)
Department of Civil Engineering, University of Patras, 26500 Patras, Greece
E-mail: nmakris@upatras.gr

N. Makris
Office of Theoretical and Applied Mechanics of the Academy of Athens, Athens, Greece

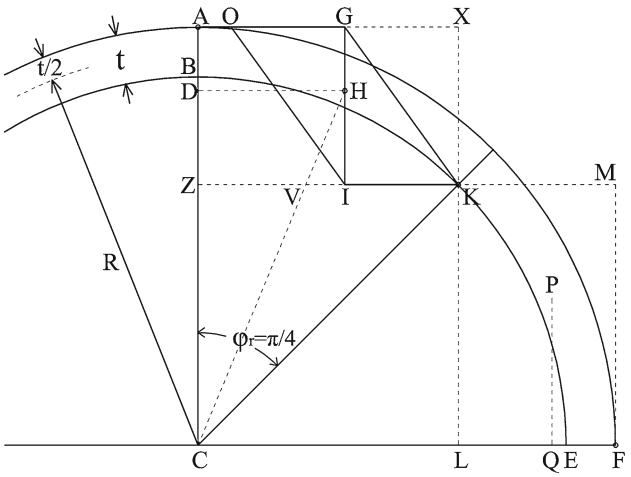


Fig. 1 Semicircular arch at its limit equilibrium state when loaded by its own weight, assuming that the internal hinge K happens at $\varphi_r = 45°$. The *horizontal* thrust at the crown, $\overrightarrow{OG}$, when added vectorially with the weight, $\overrightarrow{GI}$, of the top articulated segment, ABK of the hinged mechanism result the thrust force, $\overrightarrow{GK}$, acting on the radial rupture that generates hinge K. Clearly, the thrust force, $\overrightarrow{GK}$, is not tangent at the intrados of the arch at point K

structure are in equilibrium (Lagomarsino [4]). The masonry arch stands out as the structural system that has challenged several of the most eminent engineers and mathematicians from the second half of the seventeenth century to the beginning of the twentieth century during their efforts to develop and refine the analysis at the limit equilibrium state (Hooke [5], Gregory [6], La Hire [7,8], Bélidor [9], Couplet [10], Danyzy [11], Frézier [12], Poleni [13], Coulomb [14], Mascheroni [15], Boistard [16], Young [17,18], Lamé and Clapeyron [19], Persy [20], Navier [21], Culmann [22], Durand-Claye [23], Milankovitch [24,25] among others). Interestingly, the majority of studies on the limit equilibrium analysis of the masonry arch adopt a geometric formulation which asks for the identification of a limiting thrust line, and only a handful of studies use energy methods which are liberated from the concept of the thrust line (Mascheroni [15], Clemente [26], Sinopoli et al. [1], Ochsendorf [28], Sinopoli [27], Foce and Aita [2], Makris and Alexakis [29], Alexakis and Makris [30,31]).

As early as in the first half of the eighteenth century, Pierre Couplet [10] presented a remarkably complete solution to the problem of computing the minimum thickness of a semicircular masonry arch with mid-thickness radius, R, and thickness, t, capable of supporting its own weight. His work brings forward in a most lucid way the two key concepts needed in the limit equilibrium analysis of masonry arches that do not sustain tension: (a) the limiting thrust line and (b) the imminent mechanism of collapse.

Couplet [10] recognized that when the thickness of the semicircular arch is sufficiently small, the arch develops a five-hinge symmetric mechanism. With reference to Fig. 1—that resembles Couplet's [10] Figure—the hinges of the symmetric five-hinge mechanism develop at the extrados of the crown (point A), at the extrados of the springer (point F) and at the unknown intrados point K. The problem of determining the minimum thickness of the semicircular arch involves three unknowns: the minimum thickness, t/R, the location of the intrados hinge K and the magnitude of the horizontal thrust at point A. At that time, Pierre Couplet has only two equations available—that is moment equilibrium about the extrados hinge F at the springing and moment equilibrium about the intrados hinge K that develops at the unknown angle φ_r. So Couplet, some 50 years before the appearance of the concepts of variational calculus (Lagrange [32]), is in search of a third equation to solve the problem at hand. He by-passes this impasse by merely assuming (perhaps after being influenced by Bélidor [9]) that the location of the rupture that forms the intrados hinge K is at $\varphi_r = 45° = \pi/4$. In this way, Couplet forces the selection of the failure mechanism; therefore, his solution for the minimum thickness, $t/R = 0.101$, is unconservative, given that a neighboring mechanism might have developed at a larger thickness.

What is remarkable in Pierre Couplet's analysis is that he presents the force parallelogram of the horizontal thrust at the crown $\overrightarrow{OG}$ and the weight of the top articulated segment of the arch ABK that is $\overrightarrow{GI}$. The resultant force, $\overrightarrow{GK}$, that is the thrust force on the radial rupture that creates the intrados hinge K is clearly not tangent to the intrados of the arch. In several occasions, Pierre Couplet has been "criticized" by modern scholars for not considering a resultant thrust force $\overrightarrow{GK}$ that is tangent to the intrados, since the widely adopted analysis

during the second half of the twentieth century was formulated by incorrectly taking a thrust force $\overrightarrow{GK}$ tangent to the intrados at point K (Heyman [33–35], Bićanić et al. [36] among others).

What is also equally remarkable is that at the dawn of the twentieth century, the Serbian engineer and astronomer Milutin Milankovitch [24,25] had shown in a most lucid way that when a masonry arch forms a radial rupture, what is tangent at the intrados hinge K is the thrust line—not the thrust force at the location of the rupture. Unfortunately, Milankovitch's [24,25] seminal work remained nearly unknown until very recently (Oschendorf [28], Foce [37], Rizzi et al. [38], Makris and Alexakis [29]), and we only now recognize that Couplet's intuition for not taking the resultant thrust force, $\overrightarrow{GK}$, (shown in Fig. 1) tangent to the intrados was indeed correct! So in the absence of variational calculus back in 1730, Pierre Couplet did as well as one could possibly do to estimate the minimum thickness of a semicircular masonry arch subjected to its own weight ($t/R = 0.101$) (Fig. 2).

2 Major milestones after Couplet and before Milankovitch

Following the pioneering work of Pierre Couplet and throughout the eighteenth and nineteenth centuries, there is a growing need in Europe for masonry bridges and aqueducts. In the second half of the eighteenth century, Charles A. Coulomb is motivated from the need to develop a general theory on the stability of masonry structures, and in 1773, he publishes his seminal theory of maxima and minima (Heyman [34,39], Delbecq [40–42], Roca et al. [43] among others). Coulomb [14] without referencing the work of his compatriot Couplet [10] concludes that the most critical failure mechanism of a masonry arch is the hinge mechanism (rather than a sliding mechanism), and he is concerned with its identification. By taking an arbitrary section of the arch, Coulomb [14] calculates the maximum and minimum bounds of the horizontal thrust force, H, at the crown that is needed to keep the structure in equilibrium. For instance, if W is the weight of the portion of the arch AaMm, the condition that the arch does not hinges about points M and m is:

$$W\frac{\overline{gM}}{\overline{QM}} < H < W\frac{\overline{Gq}}{\overline{qm}} \tag{1}$$

While Coulomb [14] does not present any solution for the calculation of the exact location of the critical rupture that generates the intrados hinges, he suggests that once the calculation given by Eq. (1) is repeated

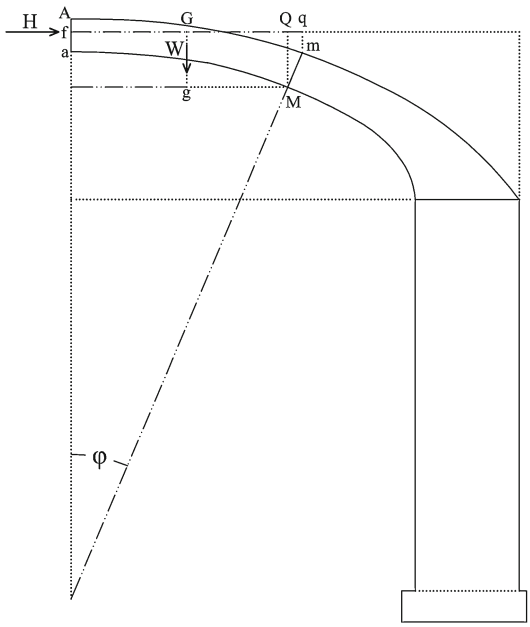


Fig. 2 The magnitude of the horizontal thrust force H at the crown is bounded from the need to satisfy moment equilibrium of the upper segment AaMm of the arch monolith about the intrados point, M, and the extrados point m. As this, exercise is repeated at various values of the angle, φ, the margin between the lower and upper bounds of the admissible *horizontal* thrust force, H, becomes narrower

at various locations, the margin between the lower and the upper bounds of the admissible horizontal thrust force becomes narrower since

$$\max H_{\min} < H < \min H_{\max} \tag{2}$$

The main contribution of C.A. Coulomb is that he recognizes the need to examine neighboring admissible mechanisms in structural mechanics, and his entire reasoning is in-line with the newly developed theory in mathematics known as calculus of variations (Lagrange [32]).

While Coulomb's [14] theory of maxima and minima derives from static equilibrium, Mascheroni [15] states that the arch has reached its limit equilibrium state when during an infinitesimal variation of the configuration of the imminent mechanism, the work of the weights of the articulated portions of the arch is zero. Mascheroni [15] considers two distinct mechanisms: (a) that corresponding to the five-hinge mechanism as identified by Couplet [10] and (b) a sliding mechanism where a center portion of the arch slides downward without friction at the imminent rupture joints and infinite friction at the springings of the arch. Clearly, Mascheroni's [15] statement that at the limit equilibrium state, the work of the corresponding weights shall be zero during an infinitesimal displacement is a clear statement of the principle of stationary potential energy—an early application of the principle of virtual work (see also Sinopoli et al. [1]).

In the early nineteenth century, the Spanish engineer Joaquin Monasterio works on the problem of determining the minimum thickness of masonry arches. His in-depth study that was unknown until recently (Huerta and Foce [44], Foce [45], Albuerne and Huerta [46]) builds upon the earlier static theory of maxima and minima developed by Coulomb [14], and he concludes that the minimum thickness of the semicircular arch needs to satisfy: $1/9 < t/R_{in} < 1/8$, where $R_{in} = R - t/2$. Monasterio's inequality for the minimum thickness of semicircular arches, $0.1053 < t/R < 0.1176$, improves Couplet's unconservative result, $t/R = 0.101$.

In the early eighteenth century, Lamé and Clapeyron [19] make an important contribution by noticing that for symmetric arches of any shape, the calculation of the location of the intrados hinge can be greatly simplified if instead of radial sections, vertical cross sections are contemplated (see also Timoshenko [47]). This is because when one takes vertical sections, the thrust force on the vertical section is indeed tangent to the resulting thrust line contrary to what happens when one takes radial sections. Lamé and Clapeyron's [19] finding that the thrust line in a masonry arch depends on the stereotomy exercised is a major step forward in the limit equilibrium analysis of masonry arches.

The multiplicity of the limiting thrust lines (*druckkurve* vs *stützlinie*) according to the stereotomy exercised was shown in a most rigorous way some eighty years later by Milutin Milankovitch [24,25].

3 Thrust line = line of resistance and funicular polygon = line of pressure

The thrust line (or *line of resistance*, Moseley [48] or *druckkurve*, Milankovitch [24,25]) is defined as the geometrical locus of the points of application of the resultant thrust force that develops at any cross section of the masonry arch. When the masonry arch consists of individual voussoirs with finite dimensions, the thrust line (line of resistance) is constructed by taking successive cuts of the arch along the physical joints of the voussoirs. For instance, consider the symmetric arch shown in Fig. 3 (top left), where $t/R = 0.12$. Starting from the vertical axis of symmetry ($\varphi = 0$), the first two voussoirs have vertical joints, and the last two voussoirs have radial joints at $\varphi = 60°\varphi = 75°$, whereas the joint between the third and the fourth voussoir is neither vertical nor radial but at an angle of 67.5°. Figure 3 (right) shows the resultant thrust forces acting on all six voussoirs of the masonry arch shown in Fig. 3 (top left) together with the projection of the thrust forces along the normal and shear direction at the joints. The choice for selecting vertical joints between the first two voussoirs is unnatural; yet, it is intentional in order to further elaborate on the idea of Lamé and Clapeyron [19], and it may be physically realizable as long as the friction coefficient along the masonry interface is sufficient ($\mu > \tan \psi_{max} = T_{2s}/T_{2n} \approx 0.84$). Furthermore, it brings forward several subtle issues pertinent to the multiplicity of the minimum thrust line and whether the thrust forces are tangent to the thrust line.

Figure 3 (bottom left) shows the free-body diagram of a portion of the arch shown in Fig. 3 (top left) which consists of the three top voussoirs. The horizontal thrust, H, at the crown of the arch is applied at the extrados of the crown given that in the entire paper we work with the minimum thrust line—that is the thrust line that passes by the extrados points A at the crown and F at the springing. The joint at the right of the third voussoir is at an angle of 67.5°, and the cut is along this angle.

Next to the free-body diagram, the force polygon of the top portion of the arch expresses graphically the equilibrium of the system. The resultant thrust T_3 at joint 3 together with its point of application is uniquely determined from force and moment equilibrium (either graphically with the force polygon or analytically by

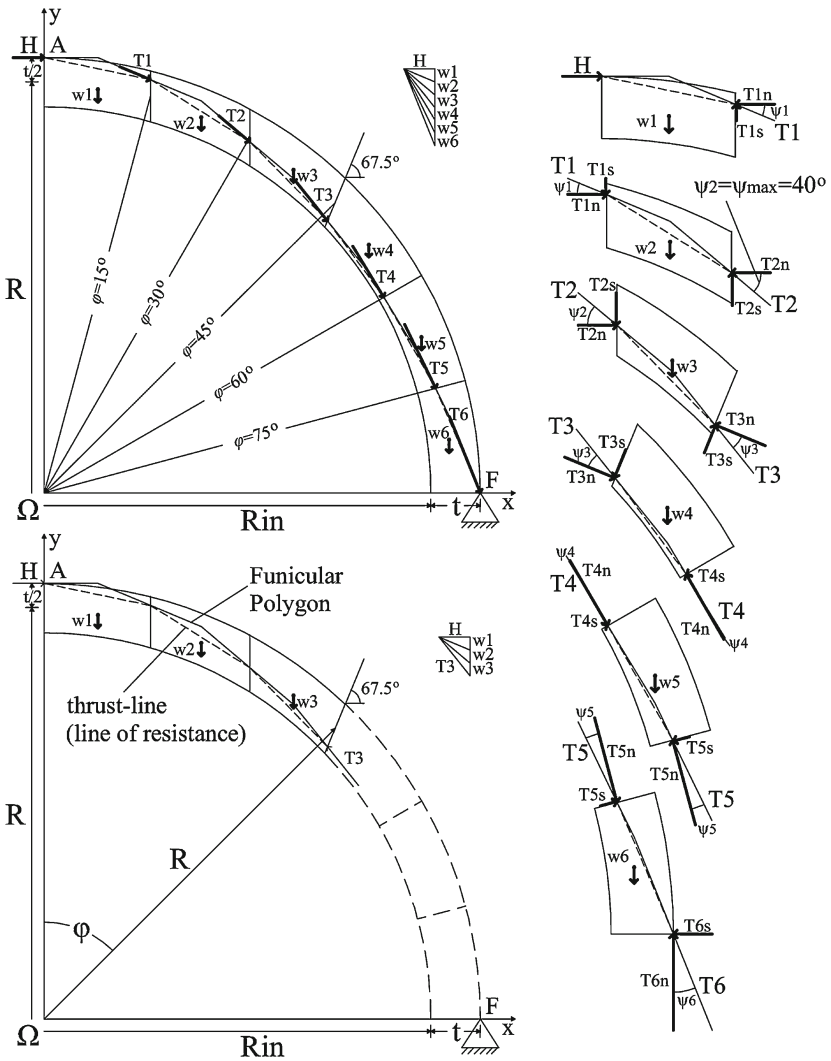


Fig. 3 Masonry arch with two vertical and two radial joints and $t/R = 0.12$. The lines of action of the resultant thrust forces T_j generate the funicular polygon shown with a *thin solid line*. *Top left*: The *thrust line* (line of resistance shown with a *dashed line*) is the geometrical locus of the points of application of the resultant thrust forces T_j acting on the physical joints. *Bottom left*: Free-body diagram of the top portion of the arch together with the corresponding force polygon. *Right*: Resultant thrust forces acting on the voussoirs together with the projections of the thrust forces along the normal and shear directions at each joint. $\tan \psi_j = T_{js}/T_{jn}$

solving equilibrium equations). This exercise is repeated at all six physical joints of the symmetric arch shown in Fig. 3 (top left), and the minimum thrust line is uniquely defined. Together with the thrust line (dashed line), Fig. 3 (top left) shows with bold line segments: (a) all the resultant thrust forces acting on the physical joints as we move from the crown to the springing of the arch and (b) the weights of the individual voussoirs. The lines of action of the resultant thrust forces generate the funicular polygon, and the lines of action of the weights of the voussoirs meet at the corners of the funicular polygon to satisfy moment equilibrium.

Figure 3 (top left) shows that the thrust line (line of resistance = geometrical locus of the application points of the resultant forces that develops at the joints of the arch) and the funicular polygon are two neighboring lines, and one may come to the conclusion that as we reduce the size of the voussoirs that these two lines will collapse to each other. Nevertheless, this in not always true, and the collapse of these two lines to a single curve depends on the stereotomy exercised on the arch—that is the directions of the physical joints when voussoirs with finite dimensions are used (Lamé and Clapeyron [19], Milankovitch [24,25], Foce [37], Makris and Alexakis [29], Alexakis and Makris [30]).

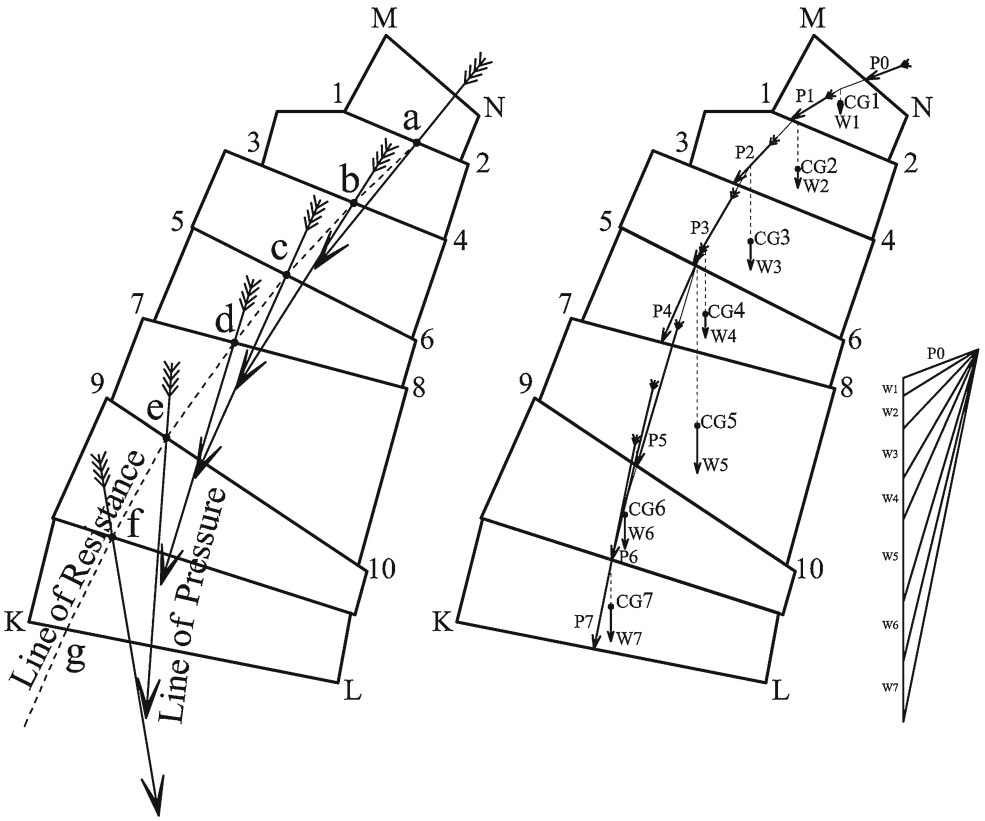


Fig. 4 *Left*: A conceptual drawing presented by Moseley [48] which distinguishes the line of resistance (*thrust line*) from the line of pressure (funicular polygon). The directions of the successive thrust forces are arbitrary without being properly proportioned according to the corresponding weights of the successive stone blocks. It is because of this random choice of the directions of the thrust forces (*arrows*) that the line of pressure (funicular polygon) seems "a slightly mysterious construct" (Heyman [35]). *Right*: The successive thrust forces are consistent with the corresponding weights of the successive stone blocks (the weights of the blocks are taken proportional to their surface) and the lines of action of the weights of the stone blocks meet at the intersection points of the lines of action of the thrust forces so that moment equilibrium is satisfied

The need to make a clear distinction between the thrust line (line of resistance) and the funicular polygon (generated from the lines of action of the resultant thrust forces acting on the physical joints) appears in the work of Moseley [48] with a drawing similar to the one appearing in Fig. 4 (left)—see also Timoshenko [47], Heyman [35], Huerta [49]. Moseley's [48] figure is merely a conceptual drawing where the directions of the successive thrust forces are arbitrary without being properly proportioned and adjusted according to the corresponding weights of the successive stone blocks that engage in the load path as it travels toward the springing of the structure. Accordingly, both the funicular polygon (line of pressure) created by the lines of action of the thrust forces (arrows) and the points of applications of these thrust forces are random in Moseley's [48] figure. It is because of this random choice of the directions of the thrust forces that the line of pressure=funicular polygon appearing in Moseley's [48] figure seems "*a slightly mysterious construct*" as reported by Heyman [35].

The stone blocks shown in Fig. 4 could be viewed as a portion of a masonry arch subject to gravity loading. If this view is taken, there is no way that the bottom most thrust force in Fig. 4 (left) passing through point f can be directed to the right of the Figure since it must always have a component to the left given that the initial force passing through point a is directed to the left and all subsequent forces that engage in the load path are vertical. The only way that the thrust force through point f can be directed to the right of the Figure is if the stone blocks are also subjected to external lateral earth pressure (see for instance Alexakis and Makris [50]).

Assuming that there is no lateral earth pressure, if one adjusts the successive thrust forces according to the corresponding weights of the successive stone blocks (the weight of the blocks are taken proportional to their surface), one obtains the physically realizable thrust forces and the associated points of application shown in

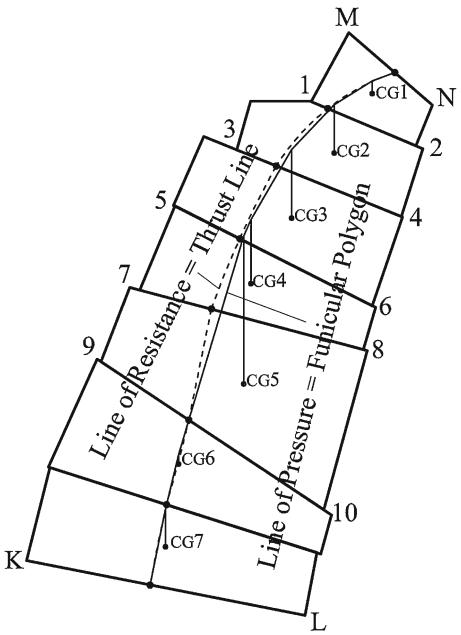


Fig. 5 Physically *realizable line* of pressure (funicular polygon) of the irregular stone-block structure presented by Moseley [48] (*continuous line*) together with the physically *realizable line* of resistance (*thrust line*) shown with *dashed line*

Fig. 4 (right). In Fig. 4 (right), the lines of action of the weights of the stone blocks meet at the intersection points of the lines of action of the thrust forces so that moment equilibrium is satisfied.

Figure 4 (right) also shows that because of the irregular shape of the stone blocks, the lines of action of two consecutive thrust forces may intersect outside the corresponding stone block. Figure 5 shows the physically realizable funicular polygon (line of pressure) of the irregular stone blocks structure presented by Moseley [48] (continuous line) together with the line of resistance (thrust line) shown with dashed line.

4 Thrust lines of an arched monolith with zero tensile strength

In the previous section, it was shown that in the case where a symmetric arch consists of a finite number of voussoirs with physical joints, the minimum thrust line is uniquely defined since equilibrium is taken on the existing physical joints. Consider now the monolithic semicircular arch shown in Fig. 6 which has zero tensile strength and therefore acts only in compression. Any point O that is located on the mid-thickness line of the arch (dashed line) has coordinates $x = R\sin\varphi$, $(0 \le x \le R)$, and $y = R\cos\varphi (0 \le y \le R)$ since the angular coordinate φ starts measuring from the vertical axis of symmetry, y. We are interested in computing the resultant thrust force acting within the arch at location O with coordinates $x = R\sin\varphi$ and $y = R\cos\varphi (0 \le \varphi \le \pi/2)$. The standard way to proceed is to make a cut passing through point O and work the force and moment equilibrium as shown in the previous section. One way to cut is along the radial direction after adopting a polar coordinate system as shown in Fig. 6 (top). With this choice, we isolate the portion of the arch ABCOD. Another way to cut is along the vertical direction after adopting a cartesian coordinate system as shown in Fig. 6 (bottom). With this choice, we isolate the portion of the arch ABCOD, which has different size and weight than the portion ABCOD; therefore, the thrust T_p along the radial cut COD is different both in magnitude and direction than the thrust T_c along the vertical cut COD. As this exercise is repeated for different points O along the mid-thickness line of the arch, one obtains two neighboring, yet, different thrust lines—one thrust line that results from radial cuts after adopting a polar coordinate system and a different thrust line that results from vertical cuts after adopting a cartesian coordinate system.

Figure 7 (left) plots these two different minimum thrust lines within a monolithic semicircular arch with $t/R = 0.12$. They have been constructed with a custom-made computer code which repeats the force equilibrium shown in Fig. 6 as point O runs from the crown to the springing. These two physically admissible thrust lines are not distinguishable in the scale of the arch; yet, if one zooms in the neighborhood isolated with the dashed parallelogram, the two thrust lines are clearly different as shown in Fig. 7 (right). Both minimum thrust

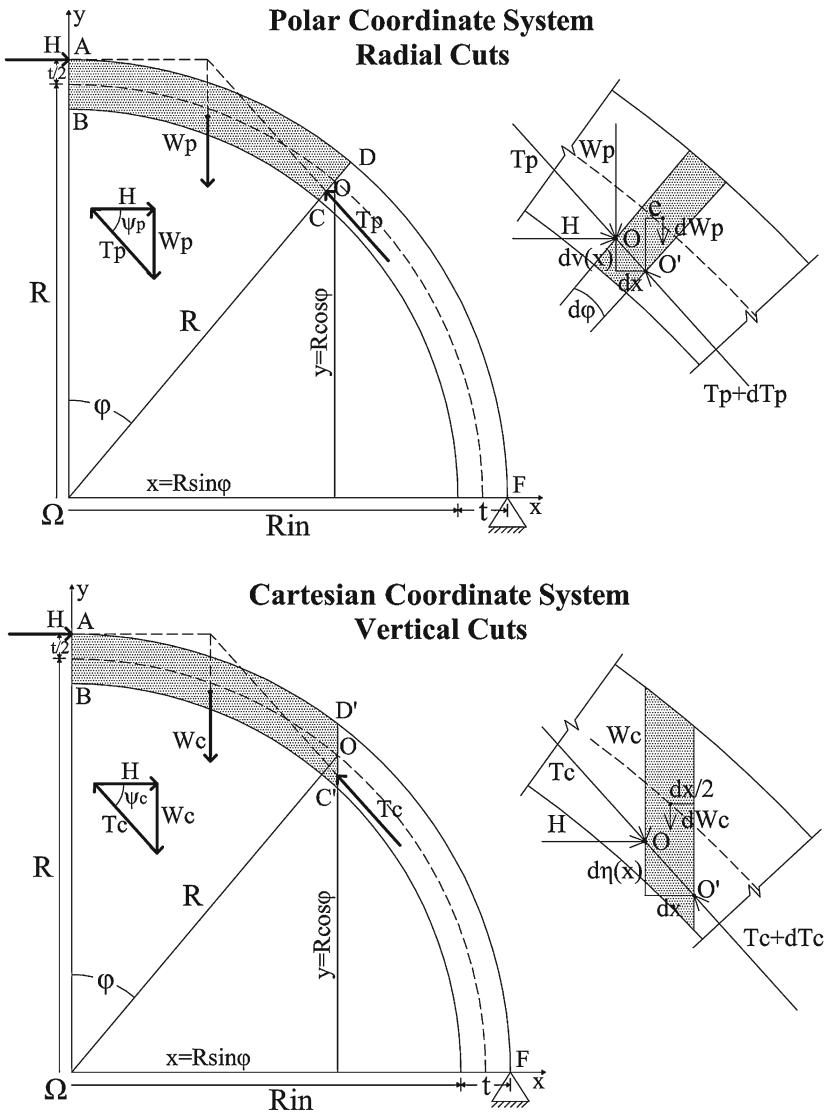


Fig. 6 Monolithic semicircular arch with zero tensile strength and $t/R = 0.12$. At any point O along the center line of the arch (*dashed line*) with polar coordinates R, φ or cartesian coordinates $x = R\sin\varphi$, $y = R\cos\varphi$, the thrust force T_p along a radial cut after adopting a polar coordinate system (*top left*) is different than the thrust force T_c along a vertical cut after adopting a cartesian coordinate system (*bottom left*). Accordingly, one obtains two distinguishable physically admissible minimum thrust lines (see Fig. 7) depending on the coordinate system that is selected. Moment equilibrium of a slice of the monolith with radial cuts (*top right*) and vertical cuts (*bottom right*)

lines are equally correct, and the fact that they lie within the physical boundaries of the arch ensures that the arch is stable. In the event that one adopts a different stereotomy (other than the radial of vertical), then a third physically admissible thrust line will emerge.

In structural engineering, the derivation of multiple solutions from equilibrium analysis is not common. The "counterintuitive" result of having different, yet, neighboring theoretically correct answers for the thrust line depending on the stereotomy exercised derives from the request to express the load path in a two-dimensional structure with finite thickness, t, with the thrust line—that is a concept inherent to a one-dimensional structure (the "hanging chain").

Alternatively, one can conduct a linear elastic analysis on the arch and identify a thrust line that is the geometrical locus of the application points of the resultant force according to the stress distribution calculated at various sections (Varma et al. [51]).

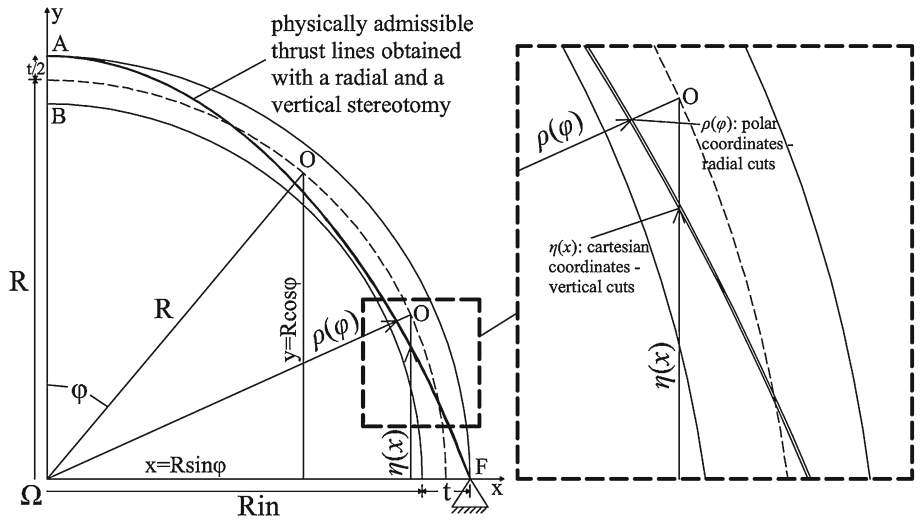


Fig. 7 Monolithic semicircular arch with the two different physically admissible *minimum thrust lines* (*left*) and $t/R = 0.12$. The two physically admissible *thrust lines* ($\rho(\varphi)$ obtained with successive radial cuts and $\eta(x)$ obtained with successive vertical cuts) are distinguishable in the enlarged parallelogram (*right*)

Interestingly, the inverted "hanging chain" (catenary) that passes from the extreme points A and F of the extrados of the arch shown in Fig. 7 offers a third line (not shown) that is different from the two minimum thrust lines—the one computed by taking radial cuts after adopting a polar coordinate system (see Fig. 6 top) and the other computed with vertical cuts after adopting a cartesian coordinate system (see Fig. 6 bottom). Recently, Makris and Alexakis [29] showed by reducing to the absurd that the catenary curve is not a physically acceptable thrust line of the semicircular arch.

4.1 Radial stereotomy and polar coordinates—Milankovitch's minimum thrust line equation

In his work of unparallel quality and rigor, Milankovitch [24,25] presents a general formulation for the thrust line of curved masonry structures. For the specific case of symmetric circular arches (as the one shown in Fig. 6), Milankovitch's formulation employs radial cuts, and after adopting a polar coordinate system, it yields a closed-form expression for the radius of curvature, ρ, of the thrust line (see also Foce [37])

$$\rho(\phi) = \frac{\rho_o H + \frac{1}{6} t\,(t^2 + 12R^2)\sin^2\frac{\phi}{2}}{H\cos\phi + tR\phi\sin\phi}. \tag{3}$$

It is worth noting that Milankovitch [24,25] obtains Eq. (3) with two different approaches: (a) via differential calculus and (b) via macroscopic equilibrium of a finite portion of the arch. Clearly, Eq. (3) is not the equation of a catenary; therefore, the questioning of whether the catenary is a physically admissible thrust line goes back to the beginning of the twentieth century.

The expression given by Eq. (3) does not assume a minimum thrust line; therefore, ρ_o is the unknown distance from the center of the circular arch to the point of application of the unknown horizontal thrust, H, acting at the crown of the arch. Among all the admissible thrust lines, the minimum thrust line passes through the extrados points A ($\varphi = 0$) at the crown and F ($\varphi = \pi/2$) at the springing of the arch. These two boundary conditions are

$$\rho(0) = \rho_o = R + \frac{t}{2} \tag{4}$$

and

$$\rho(\pi/2) = R + \frac{t}{2} \tag{5}$$

which give the value of the minimum horizontal thrust force,

$$H = tR\frac{3\pi\left(2 + \frac{t}{R}\right) - \left(12 + \frac{t^2}{R^2}\right)}{6\left(2 + \frac{t}{R}\right)}. \tag{6}$$

By feeding back the results of Eqs. (4–6) into Eq. (3), Milankovitch [24,25] obtained a remarkable closed-form expression for the radius of curvature $\rho(\varphi)$ of the minimum thrust line

$$\rho(\phi) = R\frac{3\pi\left(2+\frac{t}{R}\right)^2 - \left(2+\frac{t}{R}\right)\left(12+\frac{t^2}{R^2}\right)\cos\phi}{6\pi\left(2+\frac{t}{R}\right)\cos\phi - 2\left(12+\frac{t^2}{R^2}\right)\cos\phi + 12\left(2+\frac{t}{R}\right)\phi\sin\phi} \tag{7}$$

Equation (7) offers the expression of the minimum thrust line that passes by the extrados points A ($\varphi = 0$, crown) and F ($\varphi = \pi/2$, springing). Figure 7 plots the graph of Eq. (7) which is in full agreement with the value of the minimum thrust line calculated with the in-house software by selecting a polar coordinate system and successive radial cuts.

Returning to Fig. 3 where the two bottom voussoirs have radial joints, the radial coordinates of the application points of the thrust forces T_4 and T_5 are given precisely by Eq. (7). However, Eq. (7) does not offer the coordinates of the application points of thrust forces T_1, T_2 and T_3 since the corresponding joints are not radial.

4.2 Direction of the line of action of the resultant thrust force and the tangent to the thrust line at the point of application of the thrust force

At this point, it is worth mentioning the important conclusion derived by Milankovitch [24,25] that when a polar coordinate system is adopted (see Fig. 6 top), the slope of the thrust force $\tan\psi_p = W_p/H$ at any given point O is in general different than the slope of the thrust line $dv(x)/dx$, at that point O, where $v(x) = \rho(\varphi)\cos(\varphi)(\varphi = \arcsin(x/R))$ is the vertical coordinate of Milankovitch's thrust line given by Eq. (7) (see also Foce [37]). This can be easily shown by taking two neighboring radial cuts at angles φ and $\varphi + d\varphi$ as shown in Fig. 6 (top right). By taking moment equilibrium at the application point O of the thrust force $T_p + dT_p$, one obtains

$$-Hdv(x) + W_p dx - dW_p e = 0 \tag{8}$$

where e is the finite horizontal distance from point O to the center of gravity of the infinitesimal voussoir of the arch with weight dW_p. After dividing Eq. (8) with Hdx, one obtains

$$\tan\psi_p = \frac{W_p}{H} = \frac{dv(x)}{dx} + \frac{e}{H}\frac{dW_p}{dx} \tag{9}$$

The quantity $(e/H)\cdot(dW_p/dx)$ is a finite quantity; therefore in the case where a polar coordinate system is adopted

$$\tan\psi_p = \frac{W_p}{H} \neq \frac{dv(x)}{dx} \tag{10}$$

The above non-equality shows that in the case of radial cuts, the line of action of the resultant thrust force (funicular polygon) intersects the tangent to the thrust line (line of resistance) = geometrical locus of the application points of the resultant thrust force.

Milankovitch [24,25] further concludes that in the case of vertical cuts, one obtains the *Stützlinie* (see also Foce [37]) and the non-equality expressed by (8) becomes an equality

$$\tan\psi_c = \frac{W_c}{H} = \frac{d\eta(x)}{dx} \tag{11}$$

where $\eta(x)$ is the ordinate of the thrust line that one obtains after adopting a cartesian coordinate system.

This can be easily shown by taking two neighboring vertical cuts at abscissae x and $x + dx$ as shown in Fig. 6 (bottom right). By taking moment equilibrium at the application point O of the thrust force $T_p + dT_p$, one obtains

$$-Hd\eta(x) + W_c dx - dW_c\frac{dx}{2} = 0 \tag{12}$$

where $dx/2$ is the lever arm of the infinitesimal weight dW_c.

After dividing Eq. (12) with Hdx, one obtains

$$\tan\psi_c = \frac{W_c}{H} = \frac{d\eta(x)}{dx} + \frac{1}{2}\frac{dW_c}{H} \tag{13}$$

The quantity $dW_c/2H$ is a first-order differential that vanishes when compared with the other two finite quantities of Eqs. (11) and (13) is recovered.

The above analysis shows that when a polar coordinate system is adopted, the line of action of the resultant thrust force is in general not tangent to the thrust line given by Eq. (7), whereas when a cartesian coordinate system is adopted, the resultant thrust force at any given point is tangent to the thrust line (Makris and Alexakis [29]).

5 Limit equilibrium analysis of masonry arches with energy methods

Milutin Milankovitch [24,25] computed the correct value of the minimum thickness of the semicircular arched monolith ($t/R = 0.1075$) by assuming radial ruptures (and the associated polar coordinate system). In his analysis, he developed a geometric formulation in which the major achievement is the construction of a closed-form expression of the minimum thrust line equation. Recently, Makris and Alexakis [29] showed that Milankovitch's solution, $t/R = 0.1075$, is not unique and that it depends on the stereotomy exercised. The adoption of vertical cuts as suggested by Lamé and Clapeyron [19] in association with a cartesian coordinate system yields a neighboring minimum thrust line and a different, slightly higher value for the minimum thickness, $t/R = 0.1095$, than the value computed by Milankovitch. While Makris and Alexakis [29] succeeded in deriving the closed-form expression of the minimum thrust line when vertical cuts are assumed, the algebra and calculus involved is complicated to the extent that the geometric formulation becomes less attractive as the shape of the arch departs from the geometry of the circle. For instance, when radial ruptures are assumed, a closed-form expression for the minimum thrust line of elliptical arches is not known to the authors (see Alexakis and Makris [30]).

In parallel with the geometric formulation, Makris and Alexakis [29] formulated the limit equilibrium analysis of masonry arches by employing the principle of stationary potential energy. The main attraction of a variational formulation is that the limit equilibrium analysis is liberated from the concept of the limiting thrust line, and the result depends solely on the direction of the rupture as the collapse mechanism initiates.

The fundamental concept of a variational formulation is that among all geometric admissible states (all admissible symmetric five-hinge mechanisms), a natural state—that is a state which also satisfies equilibrium—can be detected by observing its behavior under infinitesimal geometrically admissible variations of the state. With reference to Fig. 8, the symmetric arched monolith is subject only to its own weight (no external forces), while when it assumes its minimum thickness each of the two ruptured portions of the arch hinging at point K, neither deform elastically nor dissipate energy at the hinges.

The multiplicity in the answers for the minimum thickness of the arched monolith which does not sustain tension originates from the infinite many ways that the arch may rupture when is about to form hinge K. For instance, Fig. 8 (left) shows the formation of a mechanism in an elliptical masonry arch with semispan, a, and height, b, when developing a radial rupture, whereas Fig. 8 (right) shows the formation of a mechanism in the same elliptical arch when developing a vertical rupture.

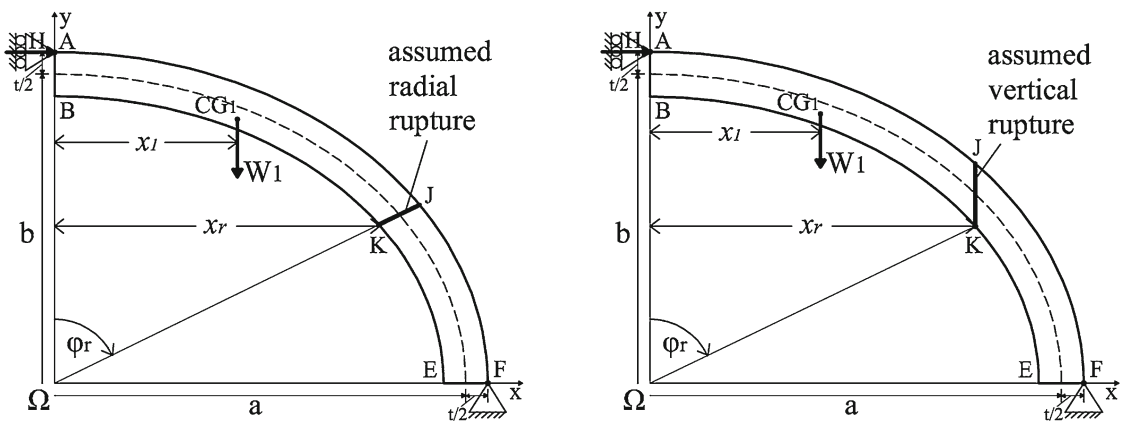


Fig. 8 Formation of a hinge mechanism in an elliptical arch by assuming that the rupture that initiates at the intrados hinge, K, develops along the radial direction (*left*) or along the vertical direction (*right*)

The structural system shown in Fig. 8 is a typical case where the only forces (weights) acting in the system are conservative and where the work of all forces is accounted by the potential energy $V(\varphi_r, b/a)$ given by (Alexakis and Makris [30])

$$V\left(\phi_r, \frac{b}{a}\right) = a^3 f\left(\phi_r, \frac{b}{a}\right)\left[\frac{1}{3}\frac{b}{a}\left(2+\frac{b}{a}\right)+\frac{1}{12}f\left(\phi_r, \frac{b}{a}\right)^2\right] \tag{14}$$

in which $f(\varphi_r, b/a) = t/a$ is a transcendental equation which derives solely by moment equilibrium of the hinged portions of the arch and relates the unknown rupture location φ_r with the unknown minimum thickness t/a of any elliptical arch described with a given height-to-semispan ration b/a.

According to the principle of stationary potential energy, the geometric admissible hinged mechanism shown in Fig. 8 is in an equilibrium state if and only if the total potential energy of the arch is stationary, i.e.,

$$\delta V\left(\phi_r, \frac{b}{a}\right) = \frac{dV\left(\phi_r, \frac{b}{a}\right)}{d\phi_r}\delta\phi_r = 0 \tag{15}$$

Substitution of Eq. (14) into Eq. (15) gives (Alexakis and Makris [30])

$$\frac{df\left(\phi_r, \frac{b}{a}\right)}{d\phi_r}\left[1+\frac{1}{4}f\left(\phi_r, \frac{b}{a}\right)^2\right] = 0 \tag{16}$$

The quantity in brackets in Eq. (16) is always positive; therefore, Eq. (16) is satisfied when $df(\varphi_r, b/a)/d\varphi_r = 0$

$$\frac{df\left(\phi_r, \frac{b}{a}\right)}{d\phi_r} = \frac{d(t/a)}{d\phi_r} = 0 \tag{17}$$

Numerical solution of the system of equations from moment equilibrium of the hinged portions of the arch (Alexakis and Makris [30]) together with Eq. (17) gives the unknown location of the rupture angle φ_r and the minimum width t/a of an elliptical arch for a given height-to-semispan ratio b/a.

Table 1 (left columns) shows the minimum thickness t/a and rupture angle $\varphi_r = \text{B}\Omega\text{K}$ for various ratios of b/a as computed with the variational formulation after adopting a radial rupture, whereas Table 1 (right columns) shows the slightly different values of the minimum thickness t/a and rupture angle $\varphi_r = \text{B}\Omega\text{K}$ as computed with the variational formulation (and also confirmed with a geometric formulation) after adopting a vertical rupture (Alexakis and Makris [30]).

Table 1 shows that the minimum thickness of an elliptical arch that is needed to support its own weight is slightly larger when one assumes vertical ruptures rather than radial ruptures, implying that the solution that corresponds to radial ruptures is unconservative. In view of this result, the question that arises is what is the direction of rupture that results to the larger value of the minimum thickness given that the minimum thickness values that results from the any other rupture direction are unconservative values.

This problem is addressed by expressing the direction of rupturing with the angle, ω, as shown in Fig. 9 and applying the principle of stationary potential energy for the entire range of ω. When $\omega = (\pi/2) - \varphi$, the

Table 1 Minimum thickness t/a and radial locations $\varphi_r = B\Omega$ K of the intrados hinge K of elliptical arches with semispan = a and height = b

b /a	Radial cuts		Vertical cuts	
	Minimum thickness: ***t/a***	Rupture angle: $\boldsymbol{\varphi_r}(^\circ)$=BΩK	Minimum thickness: ***t/a***	Rupture angle: $\boldsymbol{\varphi_r}(^\circ)$=BΩK
0.25	0.08273	84.123	0.08422	84.101
0.5	0.10127	74.442	0.10340	74.533
0.75	0.10709	64.015	0.10925	64.299
1	**0.10748**	**54.484**	**0.10946**	**54.923**
1.25	0.10513	46.567	0.10689	47.090
1.5	0.10135	40.323	0.10291	40.875
1.75	0.09684	35.516	0.09821	36.067
2	0.09200	31.857	0.09324	32.395

Bold letters are indicate the case where the masonry arch assumes the geometry of a circle

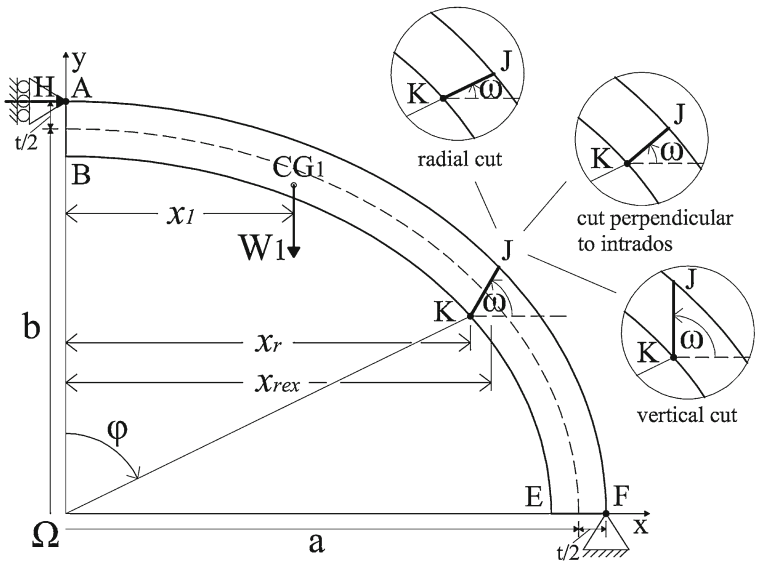


Fig. 9 Formation of a hinge mechanism in an elliptical arch where the rupture that initiates the intrados hinge, K, happens along a direction that is at an angle ω with the horizontal

rupture is radial, whereas when $\omega = \pi/2$, the rupture is vertical. In the analysis, we also consider values of $\omega > \pi/2$ in an effort to identify the most critical direction of rupture. This problem involves three unknowns: (a) the horizontal thrust force, H, at the crown, (b) the minimum thickness, t/a, of the arch and (c) the unknown location, φ_r, of the formation of the hinge K. At the same time, there are three equations available—that is moment equilibrium about hinge F and hinge K, together with Eq. (17) which originates from the application of the principle of stationary potential energy.

Moment equilibrium of the hinged mechanism about the springing hinge, F, gives the value of the minimum horizontal thrust force H at the extrados point of the crown

$$H = W \frac{3\pi\left(1+\frac{b}{a}\right)\left(2+\frac{t}{a}\right) - 8\left(1+2\frac{b}{a}+(\frac{t}{2a})^2\right)}{3\pi\left(1+\frac{b}{a}\right)\left(2\frac{b}{a}+\frac{t}{a}\right)} \tag{18}$$

in which $W = (a+b)t\pi/4$ is the weight of half the elliptical arch.

Moment equilibrium of the upper portion of the arch ABK about hinge K gives

$$H\left(b + \frac{t}{2} - y_{in}(x_r)\right) = W_1(x_r - x_1) \tag{19}$$

where H is the minimum horizontal thrust force given by Eq. (18) and W_1 and x_1 are the weight and the abscissa of the center of gravity of the upper hinged portion of the elliptical arch that is created from the rupture along the direction ω.

5.1 Case 1: $0 \le \omega \le \pi/2$

For the case where $0 \le \omega \le \pi/2$, the values of W_1 and x_1 are given by:

$$W_1 = \int_0^{x_r} y_{ex}(x)dx - \int_0^{x_r} y_{in}(x)dx + \int_{x_r}^{x_{rex}} y_{ex}(x)dx - \int_{x_r}^{x_{rex}} y_{\omega}(x)dx \tag{20}$$

and

$$x_1 = \frac{\int_0^{x_r} y_{ex}(x)xdx - \int_0^{x_r} y_{in}(x)xdx + \int_{x_r}^{x_{rex}} y_{ex}(x)xdx - \int_{x_r}^{x_{rex}} y_{\omega}(x)xdx}{W_1} \tag{21}$$

In Eqs. (20) and (21), the quantities $y_{in}(x)$ and $y_{ex}(x)$ are the ordinates of the intrados and extrados of the arch expressed in cartesian coordinates,

$$y_{in}(x) = \left(b - \frac{t}{2}\right)\sqrt{1 - \frac{x^2}{\left(a - \frac{t}{2}\right)^2}} = c_{2b}b\sqrt{1 - \frac{x^2}{(c_{2a}a)^2}} \tag{22}$$

$$y_{ex}(x) = \left(b + \frac{t}{2}\right)\sqrt{1 - \frac{x^2}{\left(a + \frac{t}{2}\right)^2}} = c_{1b}b\sqrt{1 - \frac{x^2}{(c_{1a}a)^2}} \tag{23}$$

, whereas the dimensionless quantities $c_{1a}, c_{2a}, c_{1b}, c_{2b}$ are given by

$$c_{1a} = 1 + \frac{1}{2}\frac{t}{a}, \quad c_{2a} = 1 - \frac{1}{2}\frac{t}{a}, c_{1b} = 1 + \frac{1}{2}\frac{t}{b}, \quad c_{2b} = 1 - \frac{1}{2}\frac{t}{b} \tag{24}$$

The equation of a straight line passing from the origin at an angle φ is given by

$$y_p(x) = x\cot(\phi) \tag{25}$$

and the solution of the equation

$$y_p(x) = y_{in}(x) \tag{26}$$

gives the abscissa, x_r, of the rupture point K at the intrados as function of the angle φ

$$x_r = \frac{\sqrt{\left(b - \frac{t}{2}\right)^2\left(a - \frac{t}{2}\right)^2}}{\sqrt{\left(b - \frac{t}{2}\right)^2 + \left(a - \frac{t}{2}\right)^2\cot(\phi)^2}} = a\frac{c_{2a}c_{2b}}{\sqrt{c_{2b}^2 + \frac{a^2}{b^2}c_{2a}^2\cot(\phi)^2}} \tag{27}$$

The ordinates $y_\omega(x)$ of the points along a rupture at an angle ω that initiates at the intrados at position φ are given by

$$y_\omega(x) = y_{in}(x_r) + \tan\omega(x - x_r) \tag{28}$$

while the solution of the equation

$$y_\omega(x) = y_{ex}(x) \tag{29}$$

gives the abscissa, x_{rex}, of the point J at the extrados as a function of the angle φ.

With these expressions, W_1 and x_1 given by Eqs. (20) and (21) are in terms of the polar variable φ and one may proceed with the solution of Eq. (17).

5.2 Case 2: $\omega > \pi/2$

For this case where $\omega > \pi/2$, the values of the weight W_1 and the abscissa of the center of gravity x_1 of the articulated upper portion of the arch are given by

$$W_1 = \int_0^{x_{rex}} y_{ex}(x)dx - \int_0^{x_{rex}} y_{in}(x)dx + \int_{x_{rex}}^{x_r} y_\omega(x)dx - \int_{x_{rex}}^{x_r} y_{in}(x)dx \tag{30}$$

and

$$x_1 = \frac{\int_0^{x_{rex}} y_{ex}(x)xdx - \int_0^{x_{rex}} y_{in}(x)xdx + \int_{x_{rex}}^{x_r} y_\omega(x)xdx - \int_{x_{rex}}^{x_r} y_{in}(x)xdx}{W_1}, \tag{31}$$

while the remaining calculations are the same to those presented for case 1.

Figure 10 plots the minimum thickness values, t/R (top) and the radial locations, φ_r, of the hinge K as the angle of the rupturing direction, ω, increases. Clearly, for all three configurations ($b/a = 0.5$, 1.0, and 1.5) presented in Fig. 10, the minimum thickness value is largest when $\omega = \pi/2$, that is for vertical ruptures. Interestingly, in the range $0 \le \omega \le \pi/2$, the minimum thickness value, t/R, exhibits a mild increase, whereas the radial location, φ_r, of the corresponding hinge K remains almost the same.

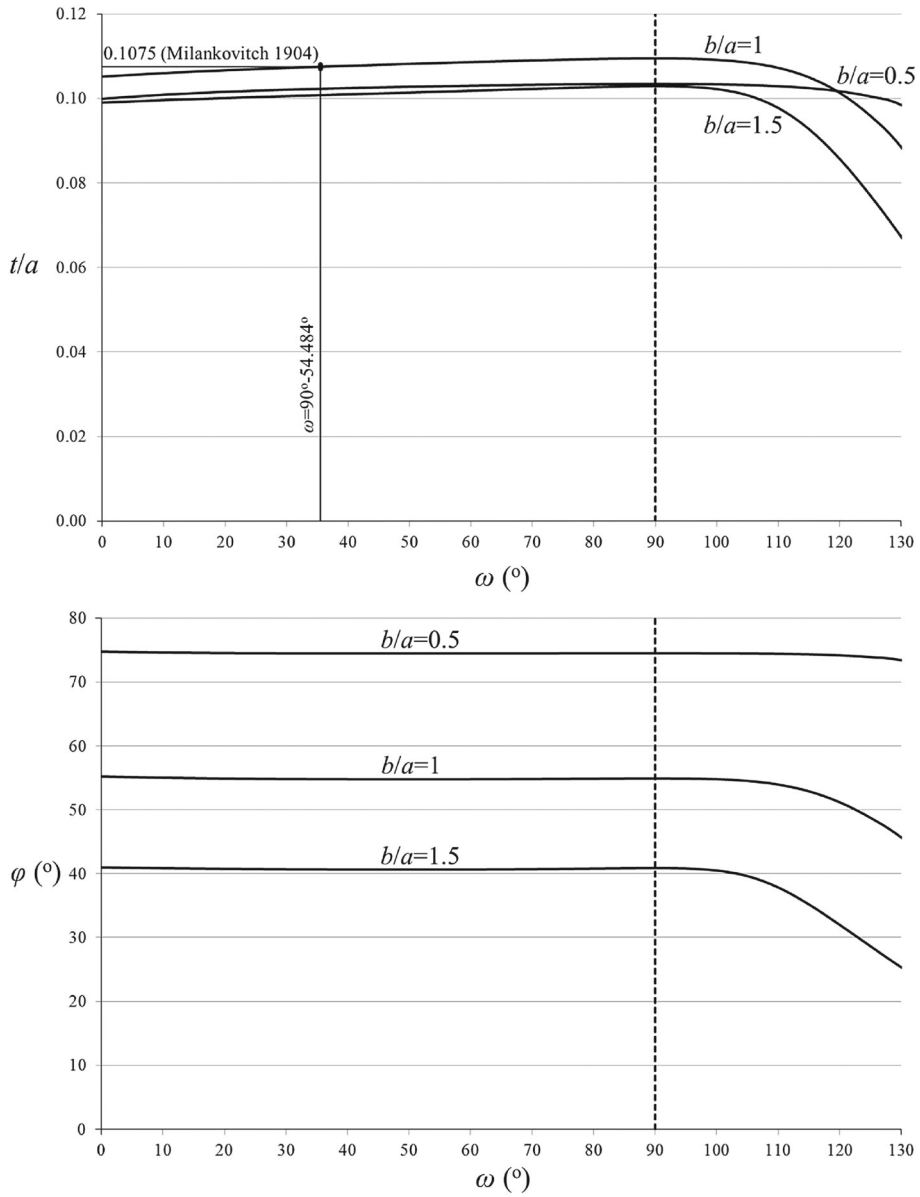


Fig. 10 Minimum thickness values, t/a (*top*), and radial locations, φ_r (*bottom*), of the hinge K shown in Fig. 9 as a function of the assumed angle of rupturing direction ω of elliptical arches with semispan, a, and height b

6 "l'expérience apprend qu'elle se dirige d'abord normalement à la courbe avec le plan de joint d'un voussoir, puis se redresse et s'élève jusqu'à l'extrados"

The variational formulation developed in this work allows for the limit equilibrium analysis of arches in which the rupture that creates the hinged mechanism is not a straight line. Several masonry arches are constructed with a layer of vitruvius voussoirs (radial joints) that follow the intrados together with additional horizontal layers of masonry above. For this kind of arches, Lamé and Clapeyron [19] have noticed that overloaded arches fail by developing a rupture that initiates radially along the physical radial joint between two adjacent vitruvius voussoirs, and subsequently, the rupture propagates upward as schematically shown in Fig. 11 that is a reproduction of Fig. 1 from Lamé and Clapeyron's [19] paper, an important publication which also offers the observation that serves as the title of this section.

Following Lamé and Clapeyron's [19] observation, we examine the limit equilibrium of an arch where the rupture is perpendicular to the intrados up to the mid-thickness of the arch, and subsequently the rupture

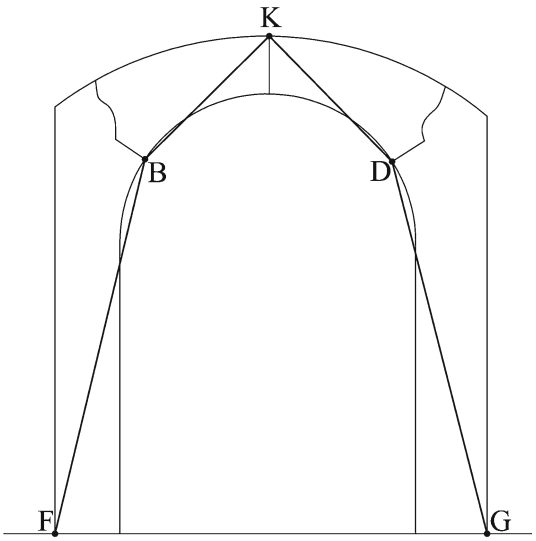


Fig. 11 Observed path of a rupture that initiates radially (points B and D) along the physical joint between two adjacent vitruvius voussoirs and subsequently it propagates upward following a nearly vertical direction

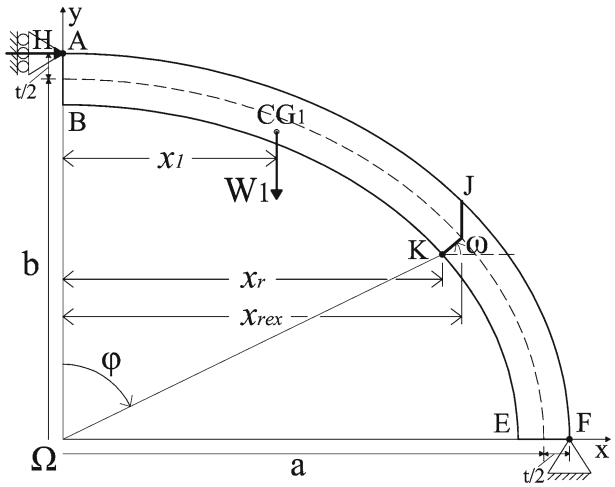


Fig. 12 Formation of a hinge mechanism in an elliptical arch by assuming that the rupture that initiates at the intrados hinge, K, develops along a *broken line* which initiates perpendicular to the intrados up to the *mid-thickness* of the arch and subsequently redirects upward propagating along the *vertical*

becomes vertical as shown in Fig. 12. When such a rupture pattern is assumed, all the equations of Sect. 5.1 are valid, except that now the abscissa of the mid-thickness point where the initial perpendicular-to-the-intrados rupture redirects along the vertical satisfies the equation:

$$y_{\omega}(x) = b\sqrt{1 - \frac{x^2}{a^2}} \tag{32}$$

The solution of Eq. (32) also gives the abscissa, $x = x_{rex}$, of the point J where the vertical rupture meets the extrados. The initial direction of rupture, ω, is perpendicular to the intrados and is expressed by

$$\omega = \arctan\left(-\frac{1}{\frac{dy_{in}(x)}{dx}|_{x=x_r}}\right) \tag{33}$$

Table 2 indicates the minimum thickness values of elliptical arches with $b/a = 0.5$, $b/a = 1$ (semicircle) and $b/a = 1.5$ as computed for the various stereotomies examined in this paper. In all three configurations,

Table 2 Minimum thickness t/a and radial locations $\varphi_r = \mathrm{B\Omega K}$ of the intrados hinge K of elliptical arches with $b/a = 0.5$, $b/a = 1$ (semicircle) and $b/a = 1.5$ for the various stereotomies examined in this paper

Rupture direction	b/a=0.5			b/a=1			b/a=1.5		
	$\omega(^\circ)$	t/a	$\varphi_r(^\circ)$	$\omega(^\circ)$	t/a	$\varphi_r(^\circ)$	$\omega(^\circ)$	t/a	$\varphi_r(^\circ)$
Radial	15.558	0.10127	74.442	**35.516**	**0.10748**	**54.484**	49.677	0.10135	40.323
Perpendicular to intrados	51.315	0.10278	74.395				26.737	0.10038	40.430
Lamé and Clapeyron's [19] observation	51.193	0.10309	74.465	35.291	0.10846	54.709	26.541	0.10163	40.659
Vertical	90.000	0.10340	74.533	90.000	0.10946	54.923	90.000	0.10291	40.875

Bold letters are indicate the case where the masonry arch assumes the geometry of a circle

the vertical stereotomy results to the largest value of the minimum thickness. Nevertheless, when there is an intrados layer of voussoirs with physical joints perpendicular to the intrados, the initial rupture has to be perpendicular to intrados (the vertical stereotomy is excluded), and the Lamé and Clapeyron [19] rupture pattern corresponds to the largest value of the minimum thickness; therefore, this rupture pattern is the most critical and explains the observation of Lamé and Clapeyron as expressed with the title of this section.

The variational method advanced in this paper is applied on the macroscopic imminent mechanism of the arch with a predetermined direction of rupturing. Clearly, the identification of the exact critical rupture pattern can only be achieved after first adopting some constitutive relations for the mechanical behavior of the joints and the masonry material and subsequently conducting a finite element analysis of the masonry structure [52–58].

7 Conclusions

This paper revisits the limit equilibrium analysis of masonry arches and explains that the infinite many neighboring solution for the minimum allowable thickness of a masonry arch result from the infinite many possible directions of rupturing that an arch with finite thickness may develop when becoming a mechanism.

Given this infinite number of physically admissible rupturing directions, the energy approach expressed with the principle of stationary potential energy emerges as the most powerful tool to analyze masonry arches at their limit equilibrium state. The paper concludes that vertical rupturing is the most critical rupturing direction since it results to the largest value of minimum thickness that an elliptical arch needs to support its own weight.

For the common case where there is an intrados layer of voussoirs with physical joints perpendicular to the intrados, the initial rupture has to be perpendicular to the intrados and the broken rupture pattern reported by Lamé and Clapeyron [19] back in 1823 corresponds to the larger value of the minimum allowable thickness; therefore, this broken rupture pattern is the most critical.

Acknowledgments This work was funded by the research project "SeismoRockBridge" No. 2295 which is implemented under the "ARISTEIA" Action of the "OPERATIONAL PROGRAMME EDUCATION AND LIFELONG LEARNING" and is co-funded by the European Social Fund (ESF) and Greek National Resources.

References

1. Sinopoli, A., Corradi, M., Foce, F.: Modern formulation for preelastic theories on masonry arches. J. Eng. Mech. **123**, 204–213 (1997). doi:10.1061/(ASCE)0733-9399(1997)123:3(204)
2. Foce, F., Aita, D.: The masonry arch between "limit" and "elastic" analysis. A critical re-examination of Durand-Claye's method. In: Proceedings of 1st International Congress on Construction History, (ed. S. Huerta, Madrid: Instituto Juan de Herrera), vol. II, pp. 895–905 (2003)
3. De Luca, A., Giordano, A., Mele, E.: A simplified procedure for assessing the seismic capacity of masonry arches. Eng. Struct. **26**, 1915–1929 (2004). doi:10.1016/j.engstruct.2004.07.003
4. Lagomarsino, S.: On the vulnerability assessment of monumental buildings. Bull Earthq. Eng **4**, 445–463 (2006). doi:10.1007/s10518-006-9025-y
5. Hooke, R.: A description of helioscopes, and some other instruments. London (1675)
6. Gregory, D.: Catenaria. Philos. Trans. R. Soc. **19**, 637–652 (1697). doi:10.1098/rstl.1695.0114
7. La Hire, P.: Traité de mécanique, où l'on explique tout ce qui est nécessaire dans la pratique des Arts, et les proprietés des corps pesants lesquelles ont eu plus grand usage dans la Physique. Imprimerie Royale, Paris (1695)

8. La Hire, P.: Sur la construction des voûtes dans les édifices. Mémoires de l'Académie Royale des Sciences, Paris (1731), pp. 69–77 (1712)
9. Bélidor, B.F.: La science des ingénieurs dans la conduite des travaux de fortification et d'architecture civile. C-A Jombert, Paris (1729)
10. Couplet, P.: De la poussée des voûtes. Histoire de l'Académie Royale des Sciences, Paris (1731, 1732), pp. 79–117 and pp. 117–141 (1729, 1730)
11. Danyzy, A.A.H.:Méthode générale pour déterminer la résistance qu'il faut oppose à la poussée des voûtes. Histoire de la Société Royale des Sciences établie à Montpellier, Lyon (1778), vol. II, pp. 40–56(1732)
12. Frézier, A.F.: La théorie et la pratique de la coupe des pierres et des bois, pour la construction des voûtes et autres parties des bâtimens civils & militaires, ou Traité de stéréotomie, à l'usage de l'architecture. 3 vols, JD Doulksseker le fils, Strasbourg, LH Guerin l'aine, Paris (1737–1739)
13. Poleni, G.:Memorie istoriche della gran cupola del tempio Vaticano e de' danni di essa, e de' ristoramenti loro. Stamperia del Seminario, Padova (1748)
14. Coulomb, C.A.: Essai sur une application des règles des maximis et minimis à quelques problèmes de statique relatifs à l'arquitecture. Mémoires de mathématique et de physique, présentés à l'académie royal des sciences per divers savants et lus dans ses assemblées, Paris (1776), vol. 7, pp. 343–382 (1773)
15. Mascheroni, L.: Nuove ricerche sull'equilibrio delle volte. Bergamo (1785)
16. Boistard, L.C.: Expériences sur la stabilité des voûtes. Recueil de divers mémoires extraits de la bibliothèque impériale des ponts et chaussées a l'usage de MM. les ingénieurs, (ed. P. Lesage), Chez Firmin Didot, Paris, vol. II, pp. 171–217 (1810)
17. Young, T.: A Course of Lectures on Natural Philosophy and the Mechanical Arts, vol. 2. Joseph Johnson, London (1807)
18. Young, T.: Bridge. Encyclopaedia Britannica (supplement to the 4th, 5th and 6th editions), Archibald Constable, Edinburgh, pp. 497–520(1824)
19. Lamé, M.G., Clapeyron, E.: Mémoire sur la stabilité des voûtes. Annales Des Mines **8**, 789–836 (1823)
20. Persy, N.: Cours sur la stabilité des constructions, à l'usage des élèves de l'école royale de l'Artillerie et du Génie. Lithographie de l'École Royale de l'Artillerie et du Génie, Metz (1825)
21. Navier, C.L.M.H.:Résumé des Leçons données à l'École des Ponts et Chaussées sur l'application de la mécanique à l'établissement des constructions et des machines. Dibot, Paris (1826)
22. Culmann, K.: Die graphische Statik. Verlag von Meyer und Zeller, Zurich (1866)
23. Durand-Claye, A.: Note sur la vérification de la stabilité des voûtes en maçonnerie et sur l'emploi des courbes de pression. Annales Des Ponts Et Chaussées **13**, 63–93 (1867)
24. Milankovitch, M.: Beitrag zur Theorie der Druckkurven. Dissertation zur Erlangung der Doktorwürde, K.K. technische Hochschule, Vienna (1904)
25. Milankovitch, M.: Theorie der Druckkurven. Zeitschrift für Mathematik Und Physik **55**, 1–27 (1907)
26. Clemente, P., Occhiuzzi, A., Raithel, A.: Limit behavior of stone arch bridges. J. Struct. Eng. **121**, 1045–1050 (1995). doi:10.1061/(ASCE)0733-9445(1995)121:7(1045)
27. Sinopoli, A.: The role of geometry in the theories on vaulted structures by Lorenzo Mascheroni. In: Proceedings of 1st International Congress on Construction History, (ed. S. Huerta, Madrid: Instituto Juan de Herrera), pp. 1865–1873(2003)
28. Ochsendorf, J.: Collapse of masonry structures. Ph.D. Dissertation, Department of Engineering, University of Cambridge, Cambridge, UK (2002)
29. Makris, N., Alexakis, H.: The effect of stereotomy on the shape of the thrust-line and the minimum thickness of semicircular masonry arches. Arch. Appl. Mech. **83**, 1511–1533 (2013). doi:10.1007/s00419-013-0763-4
30. Alexakis, H., Makris, N.: Minimum thickness of elliptical masonry arches. Acta. Mech. **224**, 2977–2991 (2013). doi:10.1007/s00707-013-0906-2
31. Alexakis, H., Makris, N.: Limit equilibrium analysis and the minimum thickness of circular masonry arches to withstand lateral inertial loading. Arch. Appl. Mech., published on line. doi:10.1007/s00419-014-0831-4 (2014)
32. Lagrange, J.L.: Mécanique analytique. Chez La Veuve Desaint, Libraire, Paris(1788)
33. Heyman, J.: The safety of masonry arches. Int. J. Mech. Sci. **11**, 363–385 (1969). doi:10.1016/0020-7403(69)90070-8
34. Heyman, J.: The Masonry Arch. Ellis Horwood, Chichester (1982)
35. Heyman, J.: La Coupe des Pierres. In: Proceedings of 3rd International Congress on Construction History, (eds. Kurrer KE, Lorenz W, Wetzk V), Neunplus1, Berlin, 2, pp. 807–812 (2009)
36. Bićanić, N., Stirling, C., Pearce, C.J.: Discontinuous modelling of masonry bridges. Comput. Mech. **31**, 60–68 (2003). doi:10.1007/s00466-002-0393-0
37. Foce, F.: Milankovitch's Theorie der Druckkurven: Good mechanics for masonry architecture. Nexus Netw. J. **9**, 185–210 (2007). doi:10.1007/s00004-007-0039-9
38. Rizzi, E., Cocchetti, G., Colasante, G., Rusconi, F.: Analytical and numerical analysis on the collapse mode of circular masonry arches. Adv. Mater. Res. **133**(134), 467–472 (2010). doi:10.4028/www.scientific.net/AMR.133-134.467
39. Heyman, J.: Coulomb's Memoir on Statics: An Essay in the History of Civil Engineering. Cambridge University Press, Cambridge (1972)
40. Delbecq, J.M.: Analyse de la stabilité des voûtes en maçonnerie de Charles Augustin Coulomb à nos jours. Annales Des Ponts Et Chaussées **19**, 36–43 (1981)
41. Delbecq, J.M.: Analyse de la stabilité des voûtes en maçonnerie par le calcul à la rupture. J. de Mécanique théorique Et appliquée **1**, 91–121 (1982)
42. Delbecq, J.M.: Les Ponts en Maçonnerie – Constitution et Stabilité. Ministère des Transports. SETRA, Paris (1982)
43. Roca, P., Cervera, M., Gariup, G., Pela', L.: Structural analysis of masonry historical constructions. Classical and advanced approaches. Arch. Comput. Methods Eng. **17**, 299–325 (2010). doi:10.1007/s11831-010-9046-1
44. Huerta, S., Foce, F.: Vault theory in Spain between XVIIIth and XIXth century: Monasterio's unpublished manuscript Nueva teorica sobre el empuje de bóvedas. In: Proceedings of 1st International Congress on Construction History, (ed. S. Huerta, Madrid: Instituto Juan de Herrera), vol. II, pp. 1155–1166 (2003)

45. Foce, F.: On the safety of the masonry arch. Different formulations from the history of structural mechanics. In: Essays in the History of Theory of Structures, (ed. S. Huerta, Madrid: Instituto Juan de Herrera), pp. 117–142 (2005)
46. Albuerne, A., Huerta, S.: Coulomb's theory of arches in Spain ca. 1800: the manuscript of Joaquín Monasterio. In: Proceedings of 6th International Conference on Arch Bridges (ARCH'10), (ed. B. Chen & J. Wei), Fuzhou, China, pp. 354–362 (2010)
47. Timoshenko, S.P.: History of Strength of Materials. McGraw-Hill Book Company, Inc., New York (1953)
48. Moseley, H.: The Mechanical Principles of Engineering and Architecture, London (1843)
49. Huerta, S.: Wedges and plate-bandes: mechanical theories after De la Hire. In: L'architrave, le plancher, la plate-forme. Nouvelle histoire de la construction, under the direction of Roberto Gargiani, PPUR Presses polytechniques et universitaires romandes, Lausanne, pp. 405–435 (2012)
50. Alexakis, H., Makris, N.: Structural stability and bearing capacity analysis of the tunnel-entrance to the stadium of ancient nemea. Int. J. Arch. Her. **7**, 673–692 (2013). doi:10.1080/15583058.2012.662262
51. Varma, M., Jangid, R.S., Ghosh, S.: Thrust line using linear elastic finite element analysis for masonry structures. Adv. Mater. Res. **133**(134), 503–508 (2010). doi:10.4028/www.scientific.net/AMR.133-134.503
52. Loo, Y.C., Yang, Y.: Cracking and failure analysis of masonry arch bridges. J. Struct. Eng. **117**, 1641–1659 (1991). doi:10.1061/(ASCE)0733-9445(1991)117:6(1641)
53. Molins, C., Roca, P.: Capacity of masonry arches and spatial frames. J. Struct. Eng. **124**, 653–663 (1998). doi:10.1061/(ASCE)0733-9445(1998)124:6(653)
54. Thavalingam, A., Bicanic, N., Robinson, J.I., Ponniah, D.A.: Computational framework for discontinuous modelling of masonry arch bridges. Comput. Struct. **79**, 1821–1830 (2001). doi:10.1016/S0045-7949(01)00102-X
55. Lourenço, P.B.: Computation on historic masonry structures. Prog. Struct. Eng. Mater. **4**, 301–319 (2002). doi:10.1002/pse.120
56. Cavicchi, A., Gambarotta, L.: Two-dimensional finite element upper bound limit analysis of masonry bridges. Comput. Struct. **84**, 2316–2328 (2006). doi:10.1016/j.compstruc.2006.08.048
57. Drosopoulos, G.A., Stavroulakis, G.E., Massalas, C.V.: Limit analysis of a single span masonry bridge with unilateral frictional contact interfaces. Eng. Struct. **28**, 1864–1873 (2006). doi:10.1016/j.engstruct.2006.03.016
58. Milani, E., Milani, G., Tralli, A.: Limit analysis of masonry vaults by means of curved shell finite elements and homogenization. Int. J. Solids Struct. **45**, 5258–5288 (2008). doi:10.1016/j.ijsolstr.2008.05.019